

# A convolutional neural network of low complexity for tumor anomaly detection

Vasileios E. Papageorgiou<sup>1</sup>[0000-0002-8131-3484], Pantelis Dogoulis<sup>2</sup>[0000-0003-3848-9927] and  
Dimitrios-Panagiotis Papageorgiou<sup>3</sup>[0000-0002-3867-7135]

<sup>1</sup> Department of Mathematics, Aristotle University of Thessaloniki, Thessaloniki, Greece  
vpapageor@math.auth.gr

<sup>2</sup> Center of Research and Technology Hellas, Thessaloniki, Greece  
dogoulis@iti.gr

<sup>3</sup> Department of Mathematics, Aristotle University of Thessaloniki, Thessaloniki, Greece  
depapage@math.auth.gr

**Abstract.** The automated detection of cancerous tumors has attracted interest mainly during the last decade, due to the necessity of early and efficient diagnosis that will lead to the most effective possible treatment of the impending risk. Several machine learning and artificial intelligence methodologies have been employed aiming to provide trustworthy helping tools that will contribute efficiently to this attempt. In this article, we present a low-complexity convolutional neural network architecture for tumor classification enhanced by a robust image augmentation methodology. The effectiveness of the presented deep learning model has been investigated based on 3 datasets containing brain, kidney and lung images, showing remarkable diagnostic efficiency with classification accuracies of 99.33%, 100% and 99.7% for the 3 datasets respectively. The impact of the augmentation preprocessing step has also been extensively examined using 4 evaluation measures. The proposed low-complexity scheme, in contrast to other models in the literature, renders our model quite robust to cases of overfitting that typically accompany small datasets frequently encountered in medical classification challenges. Finally, the model can be easily re-trained in case additional volume images are included, as its simplistic architecture does not impose a significant computational burden.

**Keywords:** Convolutional Neural Networks; Tumor Detection; Biomedical Image Classification; Data Augmentation; Entropy; Artificial Intelligence.

## 1 Introduction

Applications of artificial intelligence (AI) in medicine continue to grow and affect virtually every aspect of cancer care. These applications fall into 2 main categories, namely supervised and unsupervised learning [1-2]. In supervised learning, computers learn and adapt by studying labeled biomedical instances to copy the diagnostic skills of experienced oncologists as efficiently as possible. Three of the most common and deadly tumors that affect people's quality of life in everyday life are brain, lung, and kidney tumors, making their early detection an important concern.

A brain tumor or intracranial tumor is an abnormal mass of tissue in which cells grow unnaturally and uncontrollably. According to the World Health Organization, these

types of tumors account for less than 2% of human cancers, although their severe morbidity and associated complications make early diagnosis a very important concept in modern medicine [3]. Intracranial tumors can be fatal, worsen the patient's standard of living, and can affect men, women, or children.

Lung cancer ranks second, accounting for approximately 11.4% of total cancer cases, with an estimated 2.2 million lung cancer cases only. Lung cancer is the leading cause of death among other cancers, with deaths accounting for 18% of all cancers [4]. The survival rate of lung cancer patients 5 years after diagnosis ranges from 10 to 20%. Screening with low-dose computed tomography (CT) can help detect lung cancer at an early stage so that the disease is more responsive to treatment [5]. In general, it has been reported that the patient's chances of living a long-life increase if the cancer is detected early, diagnosed, and treated effectively [6].

Renal cell carcinoma (RCC) is the sixth most common cancer among all tumors in men and the tenth most common in women. Despite advances in understanding the molecular biology of RCC and refinements in therapies, treating patients with RCC at any stage of the disease is challenging. Diagnosis of early-stage renal cancer has improved significantly in recent decades with the widespread use of cross-sectional imaging [7]. Most renal carcinomas are initially detected as incidental renal masses on cross-sectional imaging (e.g., ultrasound, CT) performed for unspecified disease. Although most are discovered as small renal masses (70%), earlier definitive therapeutic intervention for these tumors has not resulted in a significant improvement in cancer-specific mortality [8].

Medical data analysis and disease diagnosis require a medical expert, and expert opinions often differ when analyzing medical images due to their complexity. MRI images are the most efficient medical tools for manual tumor diagnosis. They show brain tumors and contain smaller or larger regions in the cerebrum with slightly brighter colors. On the other hand, scan data from CT are usually used for the diagnosis of pulmonary nodules because they are the only ones that can show pulmonary nodules. Unlike X-ray images, they do not show lung nodules. Artificial intelligence has played an essential role in the medical field by taking advantage of the above sources that provide important information about the phenomenon under study.

In this paper, we propose a low complexity convolutional neural network (CNN) for tumor detection. The reduced complexity of the proposed network makes it ideal for studying small datasets that usually accompany medical studies, compared to many articles which utilize more complex and computationally expensive architectures. This structure not only eliminates the likelihood of overfitting, but also increases the flexibility and adaptability of the approach, as it can be re-trained without significant computational cost in the occasion where new MRI or CT images are added to the dataset. In addition, various data augmentation techniques have been implemented and their respective impact on classification efficiency has been studied in detail.

In contrast to most studies included in the literature, our novel architecture has been tested on not only one, but 3 tumor datasets. These datasets contain normal, benign and malignant instances corresponding to brain, lung and kidney tumors. Hence, the variety of different datasets and the diversity of cancer classification problems, validate the trustworthiness of the produced detection efficiency, rendering our approach a reliable medical tool that can be easily utilized in modern oncology.

## 2 Related Work

In the field of medical imaging, there are a variety of algorithms from the artificial intelligence class for brain cancer classification/detection. Characteristic examples are artificial neural networks (ANN) [9], K-nearest neighbors (KNN) [10], and support vector machines (SVM) [11-12]. In parallel, CNNs seem to be the most suitable for processing MRI or CT images due to their high classification performance. There are several articles that address binary and multiclass problems in brain tumor diagnosis using a number of state-of-the-art deep neural convolutional networks. Many articles begin their analysis with image preparation, magnification, or segmentation techniques to improve overall classification efficiency. The most relevant category of articles compared to our study corresponds to binary classification attempts of benign and malignant tumors. Seetha et al [13], Babu et al [14], Pathak et al [15], and Kulkarni et al [16] combine preprocessing and image magnification techniques with traditional CNN methods to classify benign and malignant tumors with accuracy of 97.5%, 94.1%, 98%, and 98%, respectively. In [17-19], hybrid CNN-SVM models are used for binary classification with corresponding accuracies of 88.54%, 95%, and 95.62%. Sert et al [18] and Özyurt et al [19] propose ResNet for the first part of CNN-SVM architecture, while images were preprocessed by resolution enhancement and entropy segmentation techniques. In [19], the authors compare their model with a CNN-KNN on the same dataset with an accuracy of 90.62%.

The 95% accuracy of [20] achieved by one of the three proposed CNNs is based on the ResNet50 architecture, albeit with obvious overfitting issues, as noted by Saxena et al. As mentioned earlier, there are analyzes that address multi-class classification problems using a variety of preprocessing techniques and CNNs. [21-23] propose CNN structures for classifying images representing three cases of brain tumors: Pituitary adenomas, meningiomas, and gliomas from a public dataset with accuracy of 94.39%, 90.89%, and 98%, respectively, comparing classification performance on cropped, uncropped, and segmented images. On the other hand, in [24], a Dense-Net-LSTM hybrid is used for a 4-class tumor classification problem, achieving 92.13% on a public database.

Regarding lung tumors, in [25-26] the authors use SVM classifiers and CNN GoogleNet based on the IQ-OTHNCCD dataset. In [25], the authors preprocess the images from CT using Gaussian filters, bit-plane slicing and image segmentation and achieve an accuracy of 89.88%, while in [26] they implement the Gabor filter and regions of interest (ROI) extraction with a grouping accuracy of 94.38%. Other machine learning attempts for lung cancer classification include the utilization of KNN [27], SVM [28], Naive Bayes [27], and Random Forests [29]. In [30], the authors implement CNN architectures such as VGG16, MobileNet, AlexNet, DenseNet, VGG19, and ResNet with efficiency between 48-56% for classification of normal, benign, and malignant tumors. Polat and Mehr [31] utilize a hybrid 3D CNN-SVM with a classification efficiency of 91.81%. Finally, traditional CNN methods applied to private datasets of CT images [32-33] using the median filter, contrast stretching, and Otsu segmentation are proposed.

Finally, several articles have addressed renal cancer detection, particularly using preprocessed forms of CT images. In machine learning approaches to discriminate between benign and malignant tumors [34-36], most studies focused on discriminating

between low- fat angiomyolipomas and renal cancer with promising results, with the area under characteristic curve (AUC) metric of the models reaching values between 0.90 and 0.96. On the other hand, Han et al [37], using a modified GoogleNet architecture, encountered lower performance (accuracy of 73%) on a 3-class problem for identifying papillary RCCs (pRCCs) compared to clear cell RCCs (ccRCCs) and chromophobe RCCs (chrRCCs), compared to the binary classification problem of ccRCCs compared to non-ccRCCs (accuracy of 85%). Xi et al [38] reported an increased accuracy of 70% using a ResNet network-based ensemble model that combined preoperative T2-weighted and T1 post-contrast MRI sequences and clinical variables to classify benign and malignant renal masses in 1,162 patients. Furthermore, Li et al [39] identified low- and high-grade ccRCC, respectively, based on MRI combined with patient history and radiologist-assigned imaging features and achieved an AUC of 0.845. Fenstermaker et al. [40] finally use a CNN model trained on normal and RCC tissue samples from 42 patients, while Said et al [41] implement a random forest based on features extracted from MRI images for binary classification of renal tumors.

### 3 Method

In this section we describe the complete framework that was constructed in order to train our proposed architecture and boost its generalization ability. In more detail, we analyze the source of each dataset and the classes that are contained, then we provide the proposed low complexity convolutional neural network and finally we describe the data augmentation method that was applied. We also analytically describe the basic concepts of the convolutional neural networks as well as the metrics that were used in the inference stage.

#### 3.1 Convolutional Neural Networks

Convolutional Neural Networks (CNNs) is a class of Artificial Neural Networks (ANNs) architecture that are most commonly based on the convolution kernels. These networks are mainly used in visual related problems such as video classification, image segmentation and medical image analysis. A CNN model includes the basic module of *convolutional layers* (which are the most important parts of feature extraction), *pooling layers* (which are used in order to decrease the dimensionality of the processed tensors), *batch normalization layers* (which are helpful in the computational stability during training) as well as the *fully connected layers* (which is used as the feature selection mechanism). These layers are allocated in a specific sequence, starting from the layers that are used for feature extraction and followed by the fully connected layers in order to get the final output.

Convolutional layers consist of multiple kernels which are the layers' trainable parameters, modified during each iteration. Let  $X^k \in R^{M^k \times N^k \times D^k}$  be the input of the  $k$ -th convolutional layer and  $F \in R^{m \times n \times d^k \times s}$  be an order four tensor representing the  $s$  kernels of  $k$  - th layer, of spatial span  $m \times n$ . The output of the  $k$  - th convolutional

layer will be a tensor of order 3 denoted as  $Y^k \in R^{M^k-m+1 \times N^k-n+1 \times S}$ . The elements of this tensor results from the equation

$$y_{i^k,j^k,s} = \sum_{i=0}^m \sum_{j=0}^n \sum_{l=0}^{d^k} F_{i,j,d^k,s} \times x_{i^k,j^k,l}^k. \quad (1)$$

Equation (1) is repeated for all  $0 \leq s \leq S$  and for any spatial location satisfying  $0 \leq i^k \leq M^k - m + 1$  and  $0 \leq j^k \leq N^k - n + 1$  [41].

Let  $X^k \in R^{M^k \times N^k \times D^k}$  be the input of the  $k$ -th layer that is now a pooling layer with a spatial span of  $n \times m$ . We assume that  $n$  divides  $M$  and  $m$  divides  $N$  and the stride equals the aforementioned spatial span. The output is a tensor  $Y^k \in R^{M^{k+1} \times N^{k+1} \times D^{k+1}}$ , where

$$M^{k+1} = \frac{M^k}{n}, \quad N^{k+1} = \frac{N^k}{m}, \quad D^{k+1} = D^k, \quad (2)$$

while the polling layer operates upon  $X^k$  channel by channel independently. In our network we utilize 2 max pooling layers, resulting in outputs produced based on

$$y_{i^k,j^k,d} = x_{i^k \times m + i, j^k \times n + j, d}^k \quad (3)$$

where  $0 \leq i^k \leq M^k$ ,  $0 \leq j^k \leq N^k$  and  $0 \leq d \leq D^k$ . These layers decrease the tensor's dimension, although retaining the important detected patterns [42].

On the other hand, the fully connected layers belong to the second part of a CNN aiming to efficiently select the most valuable features extracted by convolutional layers. The input of the first fully connected layer is a high dimensional vector containing all extracted features produced by a flattening operation. Finally, important transition mediums connecting the aforementioned layers are the operations of ReLU and batch normalization. The ReLU function is defined as

$$y_{i,j,d} = (0, x_{i,j,d}^k) \quad (4)$$

with  $0 \leq i \leq M^k$ ,  $0 \leq j \leq N^k$  and  $0 \leq d \leq D^k$ , aiming to transfer only the purposive elements for the classification.

Since we focus on tumor-based regions, we are processing medical images. A medical image  $X$  can be represented as a three-channel tensor (in the RGB system), formally defined as  $X \in R^{H \times W \times 3}$ , where  $H$  and  $W$  are the height and the width of the image respectively. The input tensor  $X$  corresponding to the  $i$ -th medical image is passed through the set of successive layers and a label  $y_i'$  is produced. Then an error is calculated using a defined loss function. In most cases, Cross-Entropy loss is utilized, which is denoted as  $L_{CE}$ . In our occasion, where we train our network in a binary classification scenario, we are using the Binary Cross-Entropy loss function ( $L_{BCE}$ ) which is defined as

$$L_{BCE}(y_i, y'_i) = -(y_i * \log(y'_i) + (1 - y_i) * \log(1 - y'_i)) \quad (5)$$

where  $y_i = \{0, 1\}$  corresponds to the image's ground truth. The produced error is then utilized in the learning procedure that represents the modification of the *trainable* parameters of the network based on an optimization algorithm. The majority of the analyses in the literature use Adam [41] or AdamW algorithms as optimizers.

### 3.2 Evaluation Metrics

In the inference stage, where we evaluate the performance of our training model, we use well-known measures proposed for classification related problems. These are accuracy, precision, recall and the F1 score. These are formally defined as:

$$Accuracy = \frac{TP + TN}{TP + TN + FP + FN} \quad (6)$$

$$Recall = \frac{TP}{TP + FN} \quad (7)$$

$$Specificity = \frac{TN}{TN + FP} \quad (8)$$

$$F1\ score = \frac{2TP}{2TP + FP + FN} \quad (9)$$

Accuracy denotes the percentage of the correctly classified cases from the trained model. It is the most simple and intuitive metric that can be used in the specific problem. As a general measure, *F1 score* is the harmonic mean between *Precision* and *Recall*, and high scores reflect an equally balanced model of both tumorous and non-tumorous (healthy) regions.

### 3.3 Image Processing

In this section we present the datasets that were used in our experiments as well as the augmentation-based preprocessing that was used in order to boost the model's detection ability. Finally, we revise the architecture of the low-complexity convolutional network that is previously proposed and has achieved state-of-the-art results with low computational power.

#### 3.3.1 Datasets

The brain cancer dataset contains 3000 images that can be utilized for the training and testing of the proposed CNN model. The dataset is highly balanced, where 1500 images

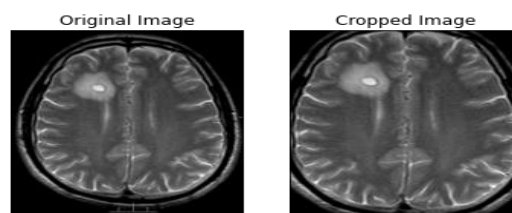
correspond to normal and 1500 images to tumorous cases. It is an open access dataset and has been uploaded on Kaggle<sup>1</sup>.

The lung cancer dataset was collected from specialists in the Iraq-Oncology Teaching Hospital/ National Center for Cancer Diseases (IQ-OTH/NCCD) over a period of three months in 2019<sup>2</sup>. It consists of 1190 images, representing CT scan slices of 110 cases (50 malignant, 15 benign and 55 normal). The dataset contains 1097 labeled images, consisting of 416 normal, 120 benign and 561 malignant cases. Since our problem is a binary-classification problem of detecting tumorous regions, we labeled as abnormal (or tumorous) all instances where benign or malignant cancer was present.

The kidney cancer dataset<sup>3</sup> was retrieved from a collection of cancer related datasets, which contains cases of brain, breast and other types of cancer. It contains 10000 images corresponding to images of 5000 normal and 5000 of tumorous cases, representing a completely balanced set.

### 3.3.2 Augmentation Pipeline

Different image-based operations were used as part of our proposed augmentation pipelines. These are *gaussian blur*, small modifications of the contrast, hue, brightness and zoom of each image (we refer to this as *color jittering*) as well as *rotation* and *translation*. *Gaussian Blur* is used as a cleaning mechanism of the image since it removes high frequencies in regions of the image and is commonly used as a denoising tool. Random *resize* ensures that the model will focus on infectious regions of the image independently of the height or the width of it. On top of that, *rotation* and *translation* will also push the model to search for the tumorous region in different areas of the image and finally *color jittering* is used in order to make the model to learn features that are not dependent on the color of each image (since there is also a variation in the pixel values among the grayscale images), but mainly on the shape of infectious and healthy regions. After the augmentation procedure, the MRI and CT images displaying brain, kidney and lung tumors are cropped automatically, aiming to remove their outer black parts that do not represent valuable information for the examined phenomenon, thus isolating the respective organ tissue that we are interested in. Fig. 1, provides some characteristic instances of the cropping process. Finally, all images are resized having a dimension of 100×100 to ensure uniformity between images.



a) Brain MRI displaying the existence of tumor

<sup>1</sup> <https://www.kaggle.com/datasets/ahmedhamada0/brain-tumor-detection>

<sup>2</sup> <https://www.kaggle.com/datasets/adityamahimkar/iqothnccd-lung-cancer-dataset>

<sup>3</sup> <https://www.kaggle.com/datasets/obulisainaren/multi-cancer>

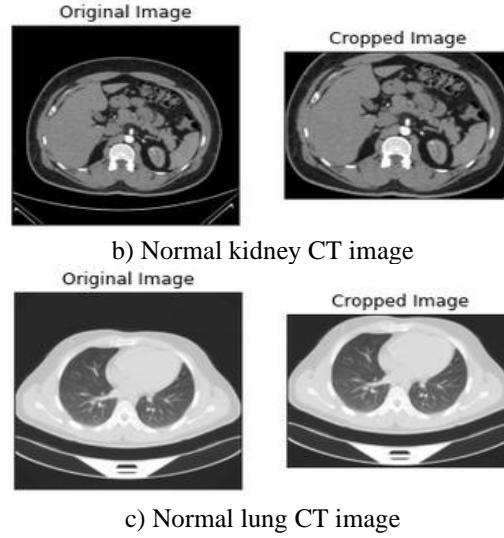


**Fig. 1.** Instances of original and cropped MRI and CT images

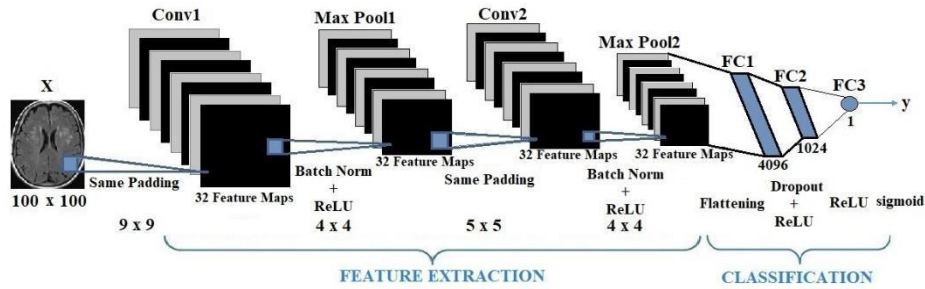


**Fig. 2.** Diagrammatic representation of the low-complexity CNN architecture

### 3.4 CNN Architecture

In this paragraph, we present a low-complexity CNN scheme including 7 main layers. The first four (2 convolutional and 2 max pooling) contribute to the feature extraction process. In addition, the 3 remaining fully connected layers take advantage of the extracted features to achieve noteworthy classification performance (Fig. 1). Two-dimensional gray-scale images of size 100×100 are placed as inputs to the proposed CNN architecture. We arrived at this choice after extensive experimentation, since the selected small input size, is accompanied by low computational burden without deteriorating the model's efficacy.

Firstly, a convolutional layer consisting of 32 kernels of 9×9 spatial span is encountered, while the extracted feature maps go through a max pooling layer of size 4×4. This pattern is replicated and contains a 5×5 convolutional and a 4×4 max pooling

layer. In both cases, *same padding* is utilized before the implementation of the convolution, while the above layers are accompanied by ReLU and batch normalization operations. The second part consists of 3 fully connected layers including 4096, 1024 and 1 node, correspondingly. Between the first, exist a dropout operation aiming to eliminate the likelihood of overfitting.

## 4 Results

The proposed low complexity scheme is employed to investigate the overall classification efficiency on all three datasets containing lung, kidney and brain tumors. For each dataset we utilized a stratified splitting strategy of ratio 70:30, before and after the implementation of the augmentation methodology, aiming to maintain balanced classes during the training and test phases. Thus, we result into test sets containing 900, 1500 and 329 images for the brain, kidney and lung datasets correspondingly.

Several learning rates were utilized during the training phase, namely  $\eta = \{0.1, 0.05, 0.01, 0.005, 0.001, 0.0005, 0.0001\}$ , while the best classification results are generated for  $\eta = 0.005$ . We trained our model for 50 epochs based on Adam optimizer, which seems to have a more unstable but more effective training process compared to other optimizers such as the stochastic gradient descent (SGD). The augmentation methodology has only been applied on the training set.

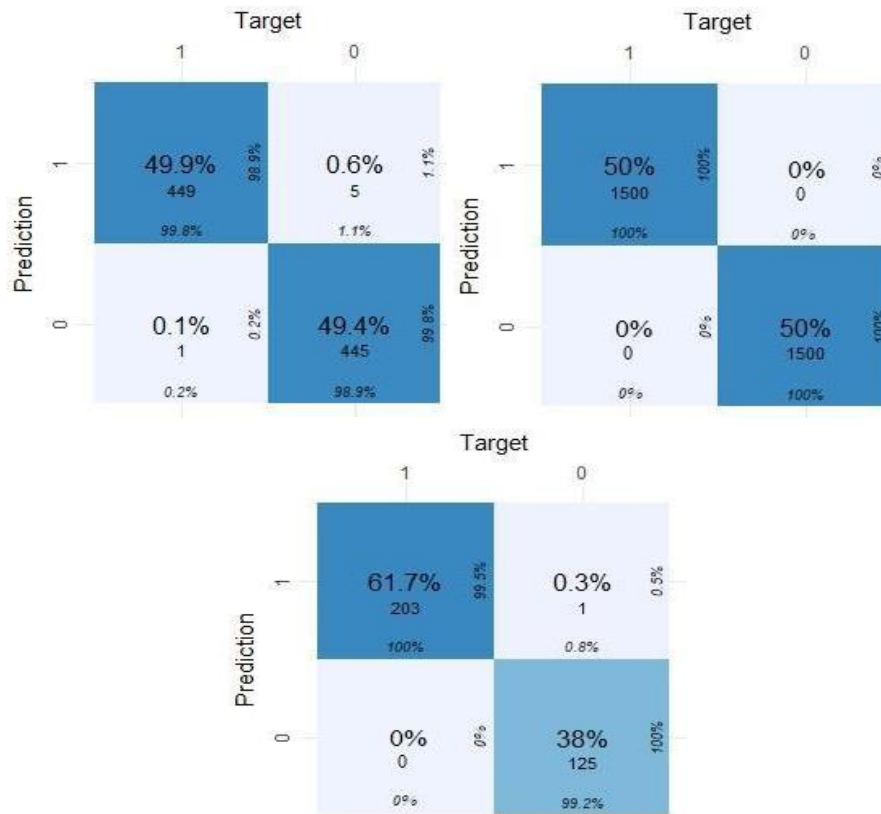
In Table 1 we observe the classification efficiency of the proposed CNN on the test set. On the other hand, Table 2 displays our model's capacity after the employment of the abovementioned augmentation pipeline. In both cases, our model presents significant tumor detection efficacy, especially for the augmented datasets, where we encounter accuracies of 99.33%, 100% and 99.7% for the brain, kidney and lung tumors respectively. Moreover, according to tables 1 and 2, kidney tumors represent the best classified type of tumors, before and after the employment of augmentation. Another important observation is the minor differentiation between the evaluation measures of specificity and recall, leading us to the conclusion that our model classifies equivalently effectively both tumorous and non-tumorous instances, regardless the cancer type.

**Table 1.** Classification performance of the low-complexity CNN based on the 3 examined datasets without augmentation

	Accuracy	Specificity	Recall	F1 score
<b>Brain Tumors</b>	98.44%	99.09%	97.88%	99.89%
<b>Kidney Tumors</b>	99.78%	96.55%	99.61%	99.78%
<b>Lung Tumors</b>	97.27%	99.11%	96.76%	98.05%

**Table 2.** Classification performance of the low-complexity CNN based on the 3 examined datasets with augmentation

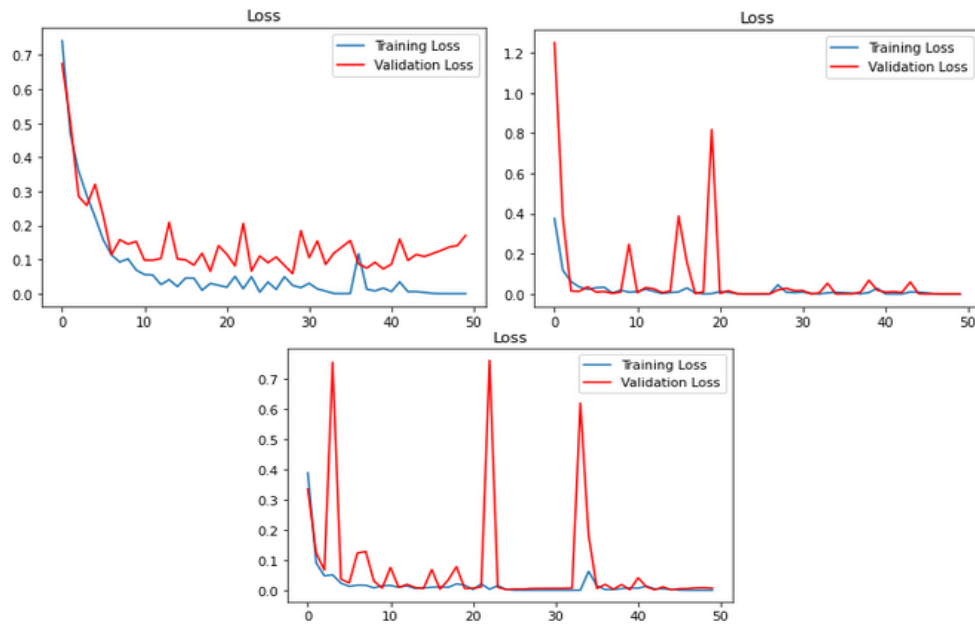
	Accuracy	Specificity	Recall	F1 score
<b>Brain Tumors</b>	99.33%	98.88%	99.78%	99.34%
<b>Kidney Tumors</b>	100%	100%	100%	100%
<b>Lung Tumors</b>	99.70%	100%	99.49%	99.74%



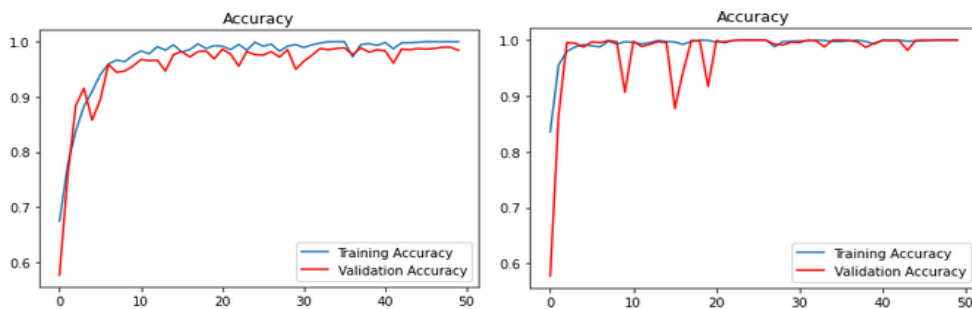
**Fig. 3.** Confusion matrices corresponding to the classification performance of the CNN after the augmentation for brain kidney and lung images

The augmentation procedure has improved the model's overall classification efficacy in all three investigated scenarios, a phenomenon that is exhibited by all 4 evaluation measures. More specifically, the testing accuracy is increased by 0.89% for brain tumors, 0.24% for kidney tumors, while the most prevalent increase is evident for lung cancer with an increase of 2.43%. In addition, we observe notable increases in the recall and the specificity regarding kidney and lung tumors of 2.73% and 3.44%, respectively.

More information about the amount of the correctly classified instances of each class is provided by the following confusion matrices (Fig. 3). These 3 matrices correspond to the presented results of table 2, concerning the case of the augmented training set. Finally, the diagrams of Fig. 4 and 5 display the evolution of the training/test losses and accuracies during the 50 epochs, showing a quite smooth training process, validating the robustness of the proposed AI model.



**Fig. 4.** Training and validation losses for the brain, kidney and lung cancer detection problem during the 50 epochs.



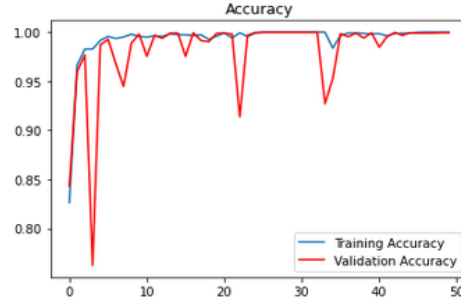


**Fig. 5.** Training and validation accuracies for the brain, kidney and lung cancer classification during the 50 epochs.

## 5 Discussion

In this article, we present a convolutional neural network scheme of low complexity for tumor anomaly detection. The limited complexity of our network renders it ideal for studying datasets including a limited number of observations, that usually accompany medical studies, compared to many papers in the literature that use more complex and computationally expensive schemes. CNNs with more convolutional and more complex fully connected layers were tested, although without improving detection accuracy. Several augmentation techniques have been applied, including Gaussian blur, color jittering, rotations, resizing and translations, while we examine their influence on the detection capability of our deep learning model. The variety of datasets and the diversity of classification challenges, enhance the robustness of the presented detection efficacy, rendering our approach a reliable medical tool.

We showed that the proposed low-complexity convolutional neural network is able to produce notably accurate results based on the 4 examined classification metrics used throughout the analysis. The selected augmentation pipeline forces the detector to learn features that focus on the tumorous regions which are independent from pixel-related features, such as the brightness or hue. The increase in the evaluation metrics is obvious, resulting in accuracy scores of 99.33%, 100.00% and 99.70% for the brain, kidney and lung cancer, respectively. On top of that, since the cardinality of the medical-related datasets is mostly limited, deep architectures may fall under the threat of overfitting [30-31]. Our low-complexity network coupled with the data augmentation overcomes this challenge and can be easily implemented under real-world circumstances, while its simplistic architecture encourages its retraining when new data is presented.

Since new types of cancer may occur, scientists should focus more on the generalization of their methods or the construction of architectures that will be able to provide robust results with limited amounts of data. Regarding future work, our objective is to take advantage of the knowledge of some deep pre-trained networks, such as ResNet50 on ImageNet, in order to create pipelines based on transfer learning and related vision techniques. It would be interesting to apply a teacher-student method to approach the problem under the few-shot or no-shot learning scenario.

## References

1. Saligkaras, D., Papageorgiou V.E.: On the detection of patterns in electricity prices across European countries: An unsupervised machine learning approach. *AIMS Energy* 10(6), 1146-1164 (2022).
2. Saligkaras, D., Papageorgiou V.E.: Seeking the Truth Beyond the Data. An Unsupervised Machine Learning Approach. *arXiv* (2022).
3. De Angelis, L.M.: Brain tumors. *New England J. Med* 344, 114-123 (2014).
4. Jassim, M.M.: Systematic review for lung cancer detection and lung nodule classification: Taxonomy, challenges, and recommendation future works. *Journal of Intelligent Systems* 31, 944-964 (2022).
5. Sung, H., Ferlay, J., Siegel, R.L., Laversanne, M., Soerjomataram, I., Jemal, A., et al.: Global cancer statistics 2020: GLOBOCAN estimates of incidence and mortality worldwide for 36 cancers in 185 Countries. *CA Cancer J Clin.* 71(3), 209-249 (2021).
6. Begum, S., Sarkar, R., Chakraborty, D., Maulik, U.: Identification of biomarker on biological and gene expression data using fuzzy preference based rough set. *J Intell Syst.* 30(1), 130-141 (2021).
7. Rasmussen, R., Sanford, T., Parwani, A.V., Pedrosa, I.: Artificial Intelligence in Kidney Cancer. *American Society of Clinical Oncology Educational Book* 42, 300-310 (2022).
8. Hollingsworth, J.M., Miller, D.C., Dignault, S., et al. Rising incidence of small renal masses: a need to reassess treatment effect. *J Natl Cancer Inst.* 98, 1331-1334 (2006).
9. Manjunath, S., Sanjay Pande, M.B., Raveesh B.N., Madhusudhan G.K. (2019). Brain Tumor Detection and Classification using Convolution Neural Network. *International Journal of Recent Technology and Engineering*, 8, 34-40.
10. Ramdlon, R.H., Kusumaningtyas, E.M., Karlita, T.: Brain Tumor Classification Using MRI Images with K-Nearest Neighbor Method. 2019 International Electronics Symposium, 660-667 (2019).
11. Vani, N., Sowmya, A., Jayamma, N.: Brain Tumor Classification using Support Vector Machine. *International Research Journal of Engineering and Technology* 4, 1724-1729 (2017).
12. Reema, M.A., Babu, A.P., et al.: Tumor detection and classification of MRI brain image using wavelet transform and SVM. 2017 International Conference on Signal Processing and Communication (ICSPC), (2017).
13. Seetha, J., Raja, S.S.: Brain Tumor Classification Using Convolutional Neural Networks. *Biomedical & Pharmacology Journal.* 11, 1457-1461, (2018).
14. Babu, K.R., Deepthi, U.S., Madhuri, A.S., Prasad, P.S., Shammem, S.: Comparative Analysis of Brain Tumor Detection Using Deep Learning Methods. *International Journal of Scientific & Technology Research* 8, 250-254 (2019).
15. Pathak, K., Pavthawala, M., et al.: Classification of Brain Tumor Using Convolutional Neural Network. *Proceedings of the Third International Conference on Electronics Communication and Aerospace Technology*, 128-132 (2019).
16. Kulkarni, S.M., Sundari, G.: Brain MRI Classification using Deep Learning Algorithm. *International Journal of Engineering and Advanced Technology* 9, 1226-1231 (2020).
17. Lang, R., Jia, K., Feng, J.: Brain Tumor Identification Based on CNN-SVM Model. *Proceedings of the 2nd International Conference on Biomedical Engineering and Bioinformatics*, 31-35 (2018).
18. Sert, E., Özyurt, F., Doğantekin, A.: A new approach for brain tumor diagnosis system: Single image super resolution based maximum fuzzy entropy segmentation and convolutional neural network. *Medical Hypotheses*, 133 (2019).

19. Özyurt, F., Sert, E., Avci, E., Doğantekin, E.: Brain tumor detection on Convolutional Neural Networks with neutrosophic expert maximum fuzzy sure entropy. *Measurement* 147, (2019).
20. Saxena, P., Maheshwari, A., Maheshwari, S.: Predictive Modeling of Brain Tumor: A Deep Learning Approach. *International Conference on Innovations in Computational Intelligence and Computer Vision*, (2020).
21. Das, S., Riaz O.F.M., Aranya, R., Labiba, N.N.: Brain Tumor Classification Using Convolutional Neural Network. *1st International Conference on Advances in Science, Engineering and Robotics Technology* (2019).
22. Afshar, P., Plataniotis, K.N., Mohammadi, A.: Capsule Networks for Brain Tumor Classification Based on MRI Images and Coarse Tumor Boundaries. *2019 IEEE International Conference on Acoustics, Speech and Signal Processing* 1368-1372 (2019).
23. Alqudah, A.M., Alquraan, H., Qasmieh, I.A., et al.: Brain Tumor Classification Using Deep Learning Technique - A Comparison between Cropped, Uncropped, and Segmented Lesion Images with Different Sizes. *International Journal of Advanced Trends in Computer Science and Engineering* 8, 3684-3691 (2019).
24. Zhou, Y., Li, Z., Zhu, H., et al.: Holistic Brain Tumor Screening and Classification Based on DenseNet and Recurrent Neural Network. *Brain lesion: Glioma, Multiple Sclerosis, Stroke and Traumatic Brain Injuries* 11383, 208-217 (2019).
25. Kareem, H.F., AL-Husieny, M.S., Mohsen, F.Y., Khalil, E.A., Hassan, Z.S.: Evaluation of SVM performance in the detection of lung cancer in marked CT scan dataset. *Indones J Electr Eng Comput Sci.* 21(3), 1731–1738 (2021).
26. Al-Huseiny, M.S., Sajit, A.S.: Transfer learning with GoogLeNet for detection of lung cancer. *Indones J Electr Eng Comput Sci.* 22(2), 1078–86 (2021).
27. Naqi, S.M., Sharif, M., Lali, I.U.: A 3D nodule candidate detection method supported by hybrid features to reduce false positives in lung nodule detection. *Multimed Tools Appl.* 78(18), 26287–6311 (2019).
28. Abbas, W., Khan, K.B., Aqeel, M., et al.: Lungs nodule cancer detection using statistical techniques. *2020 IEEE 23rd International Multitopic Conference (INMIC)*, 1–6 (2020).
29. Roy, K., Chaudhury, S.S., Burman, M., et al.: A Comparative study of lung cancer detection using supervised neural network. *2019 International Conference on Opto-Electronics and Applied Optics (Optronix)*, 1-5 (2019).
30. Mohite, A.: Application of transfer learning technique for detection and classification of lung cancer using CT images. *Int J Sci Res Manag.* 9(11), 621–34 (2021).
31. Polat, H., Mehr, H.D.: Classification of pulmonary CT images by using hybrid 3D-deep convolutional neural network architecture. *Appl Sci (Switz)* 9(5), 940 (2019).
32. Mukherjee, S., Bohra, S.U.: Lung cancer disease diagnosis using machine learning approach. *2020 3rd International Conference on Intelligent Sustainable Systems (ICISS)*, 207–11 (2020).
33. Hoque, A., Farabi, A.K.M.A., Ahmed, F., Islam, M.Z.: Automated detection of lung cancer using CT scan images. *2020 IEEE Region 10 Symposium (TENSYP)*, 1030–3 (2020).
34. Yang, R., Wu, J., Sun, L., et al.: Radiomics of small renal masses on multiphasic CT: accuracy of machine learning-based classification models for the differentiation of renal cell carcinoma and angiomyolipoma without visible fat. *Eur Radiol.* 30, 1254-1263 (2020).
35. Cui, E.M., Lin, F., Li, Q., et al.: Differentiation of renal angiomyolipoma without visible fat from renal cell carcinoma by machine learning based on whole-tumor computed tomography texture features. *Acta Radiol.* 60, 1543-1552 (2019).
36. Feng, Z., Rong, P., Cao, P., et al.: Machine learning-based quantitative texture analysis of CT images of small renal masses: differentiation of angiomyolipoma without visible fat from renal cell carcinoma. *Eur Radiol.* 28, 1625-1633 (2018).

37. Han, S., Hwang, S.I., Lee, H.J.: The classification of renal cancer in 3-phase CT images using a deep learning method. *J Digit Imaging* 32, 638-643 (2019).
38. Xi, I.L., Zhao, Y., Wang, R., et al.: Deep learning to distinguish benign from malignant renal lesions based on routine MR imaging. *Clin Cancer Res.* 26, 1944-1952 (2020).
39. Li, Q., Liu, Y.J., Dong, D., et al.: Multiparametric MRI radiomic model for preoperative predicting WHO/ISUP nuclear grade of clear cell renal cell carcinoma. *J Magn Reson Imaging.* 52, 1557-1566 (2020).
40. Said, D., Hectors, S.J., Wilck, E., et al.: Characterization of solid renal neoplasms using MRI-based quantitative radiomics features. *Abdom Radiol (NY)* 45, 2840-2850 (2020).
41. Le Cun, Y., Bengio, Y., Hinton, G.: Deep Learning. *Nature* 521, 436-444 (2015).
42. Scherer, D., Müller, A., Behnke, S.: Evaluation of Pooling Operations in Convolutional Architectures for Object Recognition. 20th International Conference on Artificial Neural Networks (2010).
43. Duchi, J.C., Hazan, E., Singer, Y.: Adaptive subgradient methods for online learning and stochastic optimization. *Journal of Machine Learning Research* 12, 2121–2159 (2011).